

K-edge resonant x-ray magnetic scattering from CoO

W. Neubeck and C. Vettier

European Synchrotron Radiation Facility, Boîte Postale 220, 38043 Grenoble Cedex, France

K.-B. Lee

Department of Physics, Pohang University of Science and Technology, Pohang 790-784, Republic of Korea

F. de Bergevin

Laboratoire Cristallographie CNRS, Boîte Postale 166, 38042 Grenoble Cedex, France

(Received 3 May 1999)

We report the observation of two contributions to resonant x-ray magnetic scattering experiments performed at the *K* edge of Co in the antiferromagnet CoO. By using polarization analysis of the scattered x-ray beam, the two resonances have been clearly associated to a quadrupolar resonance ($1s \rightarrow 3d$) and a dipolar resonance ($1s \rightarrow 4p$), respectively. The quadrupolar resonance is related to the magnetization of the $3d$ bands and to the existence of a net orbital moment, whereas the dipolar resonance must be related to spin-orbit splitting of the (empty) Co $4p$ states. [S0163-1829(99)50538-9]

Resonant x-ray magnetic scattering (RXMS) has become a widely used tool for investigations on magnetic systems. Resonant enhancement of the scattered intensity was observed by Namikawa *et al.* at the *K* edge of Ni (Ref. 1) more than 15 years ago. Subsequently, large resonant enhancements were observed in Ho,² which were explained by Hannon *et al.*³ using electronic multipole transitions between spin-orbit split core levels and available electronic states. This model gives a good qualitative description of the experimental results obtained at the $L_{2,3}$ and $M_{4,5}$ edges in lanthanide and actinide compounds. In this model the strength of the resonant enhancement is related to the spin polarization and the exchange splitting of the intermediate states. The magnetic sensitivity arises from spin-orbit coupling in the core levels or in the intermediate states. When the core level is an *s* state, the observation of magnetic resonances implies the existence of spin-orbit splitting in the intermediate states. At the *K* edge of $3d$ transition metals two processes can take place: a dipolar resonance (E1) involving the weakly polarized $4p$ levels and the quadrupolar resonance (E2) which involves the strongly polarized $3d$ bands. According to Lovesey⁴ a net orbital moment in the ground state is needed for the E2 resonance, as observed in the $L \neq 0$ system NiO.⁵ It should be noted that in $L = 0$ systems like MnO (Ref. 6) and RbMnF₃ (Ref. 7) small anomalies have been detected at the E2 resonance. In this paper we report the observation of both E1 and E2 resonances in CoO.

CoO is a simple antiferromagnet (AF), with a face-centered cubic structure above T_N ($a = 4.258$ Å, space group O_h^5). The order within an AF domain is characterized by a wave vector of the form $\{\frac{1}{2} \frac{1}{2} \frac{1}{2}\}$, so that there are four possible directions (*K* domains) for this wave vector. The moments ($3.8\mu_B$) are approximately perpendicular (82°) to their modulation direction, and lie in one of the three planes defined by the $\{111\}$ modulation and the $\{001\}$ directions.⁸ We refer to each of these moment directions as an *S* domain. There are thus twelve different but equivalent AF domains

(combination of *K*-modulation directions and *S*-moment directions), each of which possesses monoclinic symmetry. At the Néel temperature $T_N = 292$ K, CoO undergoes a large crystallographic distortion. The symmetry of this must be monoclinic also, but it consists mainly of a tetragonal component along that tetrad axis which is closest to the moment direction in a given domain.

The experiments were performed at the European Synchrotron Radiation Facility (ESRF) on ID20, the magnetic x-ray scattering beamline,⁹ which receives x rays from an undulator with 42 mm magnetic period. At 7.69 keV, a photon flux of 2×10^{12} ph/s has been measured at the sample position (for a ring current of 200 mA) with energy resolution of about 1 eV full width at half maximum (FWHM). The sample was mounted inside a closed-cycle refrigerator on a four circle diffractometer which allows polarization analysis of the scattered beam. The incoming photon beam was polarized perpendicular to the scattering plane (σ polarization). Polarization analysis of the scattered x-ray beam has been performed using Bragg scattering from a PG(006) analyzer crystal, with a peak reflectivity of 12%. The broad mosaic spread of this analyzer crystal allows proper integration of the collected intensities.

The CoO sample used in this work was a single crystal with a (001) face. At $\chi = 0$ the scattering plane contained the (001) and (010) directions. Above T_N the mosaic spread at the (002) charge reflection was 0.15° at an energy of 7.69 keV. Due to the O_h^5 symmetry, each *K* domain can be distinguished according to the propagation vector. But within each *K* domain three *S* domains contribute to the scattering. Owing to the large tetragonal distortion of CoO, associated with the spin directions, each Bragg position is split into three peaks which can be separated if the mosaic of the crystal and the resolution of the experiment is good enough. Unfortunately, several crystal grains were present in the (paramagnetic) CoO crystal and more than the three expected reflections could be found at each *K* domain position.

Nevertheless, it was possible to study the energy dependence of the magnetic intensity for a number of reflections.

In the described experiment, eleven different magnetic positions in reciprocal space have been studied. At each position several peaks have been found, belonging to different S domains as well as different grain orientations. For the resonant studies the two most intense peaks, one near the $(\frac{1}{2} \frac{1}{2} \frac{5}{2})$ position and the other one near the $(\frac{1}{2} \frac{1}{2} \frac{7}{2})$, were chosen. They belong to the same K domain $(\frac{1}{2} \frac{1}{2} \frac{1}{2})$. No scattered intensity could be detected at those positions at temperatures above T_N . The magnetic intensity was measured in both polarization channels, $\sigma\sigma$ and $\sigma\pi$, as a function of energy (7.65 keV – 7.75 keV, Co K edge at 7.709 keV). The polarization analysis is used to discriminate between E1 and E2 resonant process, as the scattering amplitude contains different geometrical factors for the two processes.^{3,10} The E1 scattering amplitude is proportional to:

$$f_{E1} \propto i(\hat{\epsilon}_f \times \hat{\epsilon}_i) \cdot \hat{z} \quad (1)$$

with $\hat{\epsilon}_f$ and $\hat{\epsilon}_i$ being the direction of polarization of the outgoing and incoming photon beam and \hat{z} the direction of the magnetic moments. This geometrical factor gives a finite contribution to the $\sigma\pi$ polarization channel, but no contribution to the $\sigma\sigma$ channel. The geometrical factor of the E2 resonant process has a more complicated dependence in $\hat{\epsilon}_f$, $\hat{\epsilon}_i$, \hat{z} and the wave vectors of the incoming and outgoing beam; its complete development can be found in the literature.¹⁰ In contrast with the E1 process, the scattering amplitude in an E2 process is nonzero in both polarization channels.

The scattered intensities presented in this work are all integrated intensities taken from rocking curves and normalized to the intensity of a monitor in front of the diffractometer. The absorption coefficient μ has been deduced from fluorescence measurements¹¹ performed on the same sample. Since absorption effects become extremely important in the vicinity of the K edge, we have included the absorption corrections in the model used to simulate the experimental data.

The key results of our work are described in Figs. 1 and 2, which represent the scattered magnetic intensity as a function of energy at the two different magnetic positions in reciprocal space. In the upper graph, we represent the measured intensity of the $\sigma\pi$ channel and the lower graph shows the $\sigma\sigma$ channel.

First let us concentrate on the $(\frac{1}{2} \frac{1}{2} \frac{5}{2})$ reflection (Fig. 1). At 7.707 keV, the intensity is enhanced by approximately a factor of 4 over the nonresonant signal seen at lower energy. The constant nonresonant magnetic scattering interferes with the resonant magnetic scattering in the vicinity of the K edge, which results in an increase of the intensity at lower (higher) energy and a dip in the intensity at higher (lower) energies in the $\sigma\pi$ ($\sigma\sigma$) polarization channel. Above the edge, the nonresonant magnetic scattering becomes weaker due to higher absorption, but is still measurable. The presence of the enhancement in both polarization channels identifies this resonance at 7.707 keV clearly as an E2 ($1s \rightarrow 3d$) type resonance. This is further supported by

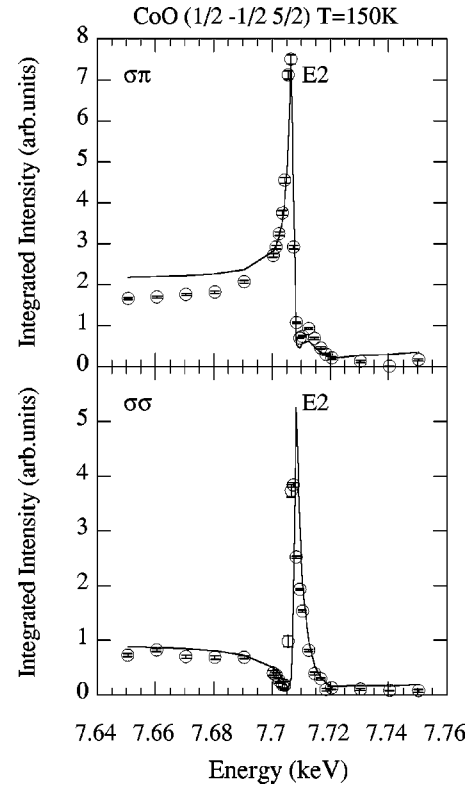


FIG. 1. The magnetic scattered intensity at the $(\frac{1}{2} \frac{1}{2} \frac{5}{2})$ magnetic Bragg peak as a function of photon energy. The upper graph shows the scattered intensity in the $\sigma\pi$ channel, whereas the lower graph shows the intensity measured in the $\sigma\sigma$ channel. The resonant enhancement of the scattered intensity at 7.709 keV originates from quadrupolar transitions ($1s \rightarrow 3d$), as the enhancement is present in both polarization channels. The solid lines are simulations, discussed in the text.

the observation of a preedge feature at 7.707 keV in the absorption measurement (see Fig. 3), which is associated with $1s \rightarrow 3d$ transitions.

The energy dependence of the magnetic intensity is very different at the second reflection $(\frac{1}{2} \frac{1}{2} \frac{7}{2})$. In the $\sigma\pi$ channel two distinct resonances were observed. The first one is found at the E2 energy position of 7.707 keV similarly to the $(\frac{1}{2} \frac{1}{2} \frac{5}{2})$ reflection; it also appears in the second polarization channel, confirming its E2 character. The second resonance is found at higher energy at 7.724 keV. Since this second enhancement is not observed in the $\sigma\sigma$ channel it is identified as an E1 transition $1s \rightarrow 4p$. The E1 resonant peak is significantly broader (FWHM ~ 5.5 eV) in energy than the E2 resonant peak (FWHM ~ 1 eV), in agreement with the $4p$ bands being wider in energy than the $3d$ bands. In the $\sigma\sigma$ channel at the $(\frac{1}{2} \frac{1}{2} \frac{7}{2})$ reflection, the resonant intensity at the E2 position is three times higher than at the $(\frac{1}{2} \frac{1}{2} \frac{5}{2})$ position, whereas the nonresonant magnetic intensity at the $(\frac{1}{2} \frac{1}{2} \frac{7}{2})$ position is lower than at the $(\frac{1}{2} \frac{1}{2} \frac{5}{2})$ position (see Figs. 1 and 2).

To emphasize the actual resonant enhancement at E1, we display in Fig. 3 the measured intensity in the $\sigma\pi$ channel after correction for absorption.¹¹ The relative enhancement of the corrected magnetic intensity at the E1 position com-

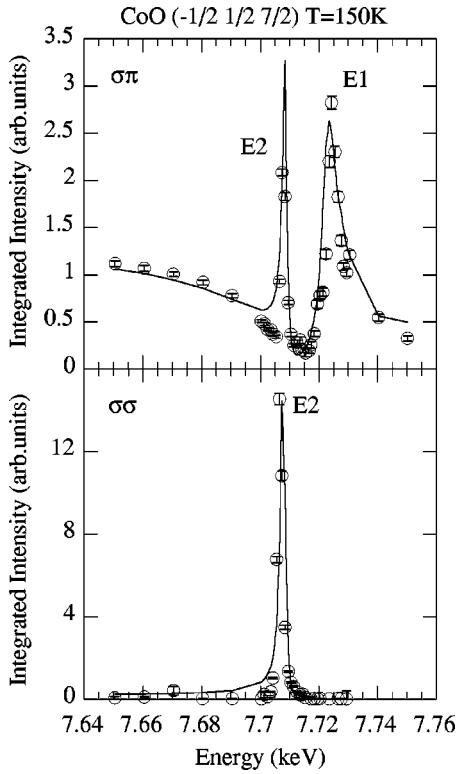


FIG. 2. The magnetic scattered intensity at the $(\frac{1}{2} \frac{1}{2} \frac{7}{2})$ magnetic Bragg peak as a function of photon energy. The upper graph shows the scattered intensity in the $\sigma\pi$ channel, whereas the lower graph shows the intensity measured in the $\sigma\sigma$ channel. The energy line shape for this reflection is more complicated, due to the presence of a dipolar resonance ($1s-4p$), which is only observable in the rotated $\sigma\pi$ polarization channel. The solid lines are simulations, discussed in the text.

pared to the nonresonant intensity is a factor of 16, which is much more important than the relative enhancement of a factor of 1.6 at the E2 resonance.

The absence of an E1 resonance at the $(\frac{1}{2} \frac{1}{2} \frac{5}{2})$ reflection can be understood when taking into account the magnetic structure⁸ and the crystal orientation, which enter the geometrical factor of the E1 scattering amplitude. Using the Herrmann-Ronzaud⁸ model for the magnetic moment directions of CoO, the factor $|\hat{\epsilon}_f \times \hat{\epsilon}_i \cdot \hat{z}|^2$ is at least ten times smaller for the S domain for which the magnetic moment direction is characterized by the (001) axis, compared to the two other S domains. In addition absorption becomes important at the E1 energy position and thus the E1 resonant intensity becomes too weak to be detected for this reflection. On the other hand at the $(\frac{1}{2} \frac{1}{2} \frac{7}{2})$ reflection a strong E1 resonance is expected for the S domain with the magnetic-moment direction characterized by the (001) axis.

Now we consider the energy line shape. The magnetic scattering amplitude near an absorption edge is the sum of the nonresonant scattering amplitude and resonant terms from the E2 and E1 contributions:

$$f_{mag} = i(f_{nonres} + f_{res}^{E2} + f_{res}^{E1}) = iA \left(1 + \frac{B}{x_{3d} - i} + \frac{C}{x_{4p} - i} \right), \quad (2)$$

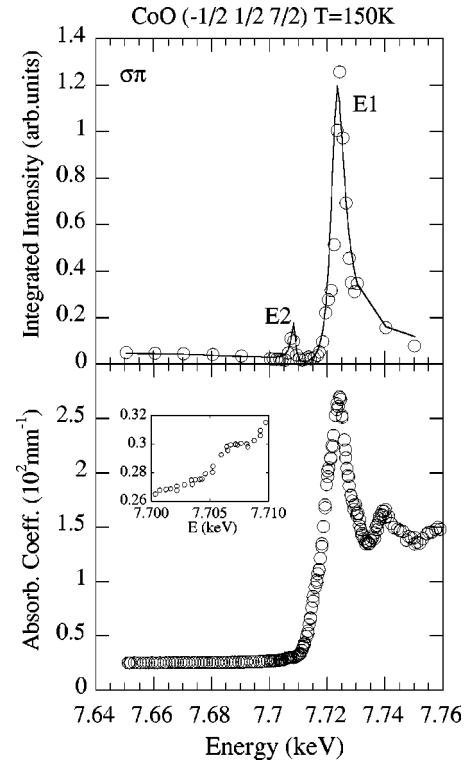


FIG. 3. The upper figure shows the absorption corrected intensities for the $(\frac{1}{2} \frac{1}{2} \frac{7}{2})$ reflection in the $\sigma\pi$ channel. It can be seen that after absorption correction the E1 resonant enhancement is much more important than the E2 one. The lower figure shows the linear absorption coefficient of CoO determined from the fluorescence measurement. The inset shows the weak anomaly at the E2 resonant energy.

where A is the amplitude of the nonresonant, and B and C the relative enhancement of the E2 and E1 processes compared to the nonresonant scattering (including geometrical factors). x describes the deviation from resonance in units of the core-hole lifetime, $x_i = (E_{c_i} - E_a - \hbar\omega)/(\Gamma/2)$, where $E_{c_i} - E_a$ is the resonant energy. Experimentally, the core-hole lifetime Γ was found to be 1.7 eV from fluorescence measurements.¹² This value includes the energy resolution broadening.

The scattered intensities are proportional to the modulus squared of the scattering amplitude:

$$I_{mag}^{\sigma\pi} \propto \left[1 + B_\pi \left(\frac{x_{3d}}{x_{3d}^2 + 1} \right) + C \left(\frac{x_{4p}}{x_{4p}^2 + 1} \right) \right]^2 + \left[B_\pi \left(\frac{1}{x_{3d}^2 + 1} \right) + C \left(\frac{1}{x_{4p}^2 + 1} \right) \right]^2, \quad (3)$$

$$I_{mag}^{\sigma\sigma} \propto \left[1 + B_\sigma \left(\frac{x_{3d}}{x_{3d}^2 + 1} \right) \right]^2 + \left[B_\sigma \left(\frac{1}{x_{3d}^2 + 1} \right) \right]^2. \quad (4)$$

The subscripts π and σ indicate that the geometrical factors contained in the scattering amplitudes of the nonresonant and E2 process are different in the two polarization channels.

In order to simulate the broader $4p$ bands we have assumed a larger Γ , which of course is a very crude model. More sophisticated models should take into account the band-like nature of Co $4p$ states. At the $(\frac{1}{2}\frac{1}{2}\frac{5}{2})$ reflection, this modeling provides the following relative scattering amplitudes: $B_\sigma=2.2$ and $B_\pi=-1.6$, and at the $(\frac{1}{2}\frac{1}{2}\frac{7}{2})$ reflection: the E2 amplitudes $B_\sigma=18$ and $B_\pi=-1.8$. Its E1 amplitude C is found to be $C=4.2$. These relative scattering amplitudes (with signs) are in agreement with the predictions of the geometrical factors contained in the scattering amplitudes of the nonresonant and resonant processes for the same S domains as discussed for the E1 resonance. This internal consistency supports the validity of our modeling.

In conclusion, we have reported the observation of resonant x-ray magnetic scattering at the K edge of Co in the antiferromagnet CoO. Two distinct resonances have been observed and it is shown that they can be attributed to quadrupolar transitions to the magnetic $3d$ levels and dipolar transitions to the $4p$ bands. The origin of the E2 resonance arises

from the polarization of the $3d$ states. As developed by Lovesey⁴ the presence of an E2 resonance indicates the existence of a significant orbital momentum contribution to the total magnetization density, whereas in compounds without orbital moment, such as RbMnF_3 ,⁷ only small anomalies are observed. In CoO a strong orbital moment of the order of $L\sim 1\mu_B$ has been invoked to describe its insulating character.^{13,14} The observation of the E1 resonance is somehow surprising as the $4p$ bands of Co in CoO are supposed to be empty. The origin of the dipolar amplitude must arise from the spin-orbit splitting of the Co $4p$ states accompanied by an exchange splitting.⁷ Such splittings lead to a magnetic sensitivity which is in fact comparable to that observed in rare earths at the $L_{2,3}$ edge; however the resonant amplitude at the E1 threshold, which involves empty $4p$ states, deserves further theoretical treatment based on band calculations.

We are indebted to J. Baruchel for providing us with CoO crystals.

¹K. Namikawa, M. Ando, T. Nakajima, and H. Kawata, J. Phys. Soc. Jpn. **54**, 4099 (1985).

²D. Gibbs, D.R. Harshman, E.D. Isaacs, D.B. McWhan, D. Mills, and C. Vettier, Phys. Rev. Lett. **61**, 1241 (1988).

³J.P. Hannon, G.T. Trammel, M. Blume, and D. Gibbs, Phys. Rev. Lett. **61**, 1245 (1988).

⁴S.W. Lovesey, J. Phys.: Condens. Matter **10**, 2505 (1998).

⁵J.P. Hill, C.-C. Kao, and D.F. McMorrow, Phys. Rev. B **55**, R8662 (1997).

⁶W. Neubeck, C. Vettier, F. de Bergevin, and D. Mannix (unpublished).

⁷A. Stunault, F. de Bergevin, D. Wermeille, C. Vettier, T. Brückel, N. Bernhoeft, G. McIntyre, and J. Y. Henry, Phys. Rev. B (to be published 1 October 1999).

⁸D. Herrmann-Ronzaud, P. Burlet, and J. Rossat-Mignod, J. Phys.

C **11**, 2123 (1978).

⁹A. Stunault, C. Vettier, F. de Bergevin, N. Bernhoeft, V. Fernandez, S. Langridge, E. Lidstroem, J.E. Lorenzo-Diaz, D. Wermeille, L. Chabert, and R. Chagnon, J. Synchrotron Radiat. **5**, 1010 (1998).

¹⁰J. Hill and D.F. McMorrow, Acta Crystallogr., Sect. A: Found. Crystallogr. **A52**, 236 (1996).

¹¹K. Dumesnil, A. Stunault, Ph. Mangin, C. Vettier, D. Wermeille, N. Bernhoeft, S. Langridge, C. Dufour, and G. Marchal, Phys. Rev. B **58**, 3172 (1998).

¹²F. de Bergevin, M. Brunel, R.M. Galéra, C. Vettier, E. Elkaïm, M. Bessière, and S. Lefebvre, Phys. Rev. B **46**, 10 772 (1992).

¹³A. Svane and O. Gunnarsson, Phys. Rev. Lett. **65**, 1148 (1990).

¹⁴T. Shishidou and T. Jo, J. Phys. Soc. Jpn. **67**, 2637 (1998).